Journal of Autoimmunity 39 (2012) 428–440

Contents lists available at SciVerse ScienceDirect

Journal of Autoimmunity

journal homepage: www.elsevier.com/locate/jautimm

Nuclear orphan receptor NR2F6 directly antagonizes NFAT and RORγt binding to the *Il17a* promoter

Natascha Hermann-Kleiter [a,*], Marlies Meisel [a], Friedrich Fresser [a], Nikolaus Thuille [a], Mathias Müller [b], Lukas Roth [b], Andreas Katopodis [b], Gottfried Baier [a,*]

[a] Department for Pharmacology and Genetics, Medical University Innsbruck, Peter Mayr Str. 1a, A-6020 Innsbruck, Austria
[b] Novartis Institute for BioMedical Research, Basel, Switzerland

ARTICLE INFO

Article history:
Received 25 June 2012
Received in revised form
19 July 2012
Accepted 19 July 2012

Keywords:
Autoimmunity
CD4+ Th17 cells
Il17a promoter
NR2F6
NFAT
RORγt

ABSTRACT

Interleukin-17A (IL-17A) is the signature cytokine produced by Th17 CD4+ T cells and has been tightly linked to autoimmune pathogenesis. In particular, the transcription factors NFAT and RORγt are known to activate *Il17a* transcription, although the detailed mechanism of action remains incompletely understood. Here, we show that the nuclear orphan receptor NR2F6 can attenuate the capacity of NFAT to bind to critical regions of the *Il17a* gene promoter. In addition, because NR2F6 binds to defined hormone response elements (HREs) within the *Il17a* locus, it interferes with the ability of RORγt to access the DNA. Consistently, NFAT and RORγt binding within the *Il17a* locus were enhanced in *Nr2f6*-deficient CD4+ Th17 cells but decreased in *Nr2f6*-overexpressing transgenic CD4+ Th17 cells. Taken together, our findings uncover an example of antagonistic regulation of *Il17a* transcription through the direct reciprocal actions of NR2F6 versus NFAT and RORγt.

1. Introduction

CD4+ Th17 cells are important for immune defense against bacteria and fungi [1]. Moreover, this T cell subset produces the proinflammatory effector cytokines interleukin (IL)-17A and IL-17F, which are involved in tissue inflammation and contribute to

focused on a detailed mechanistic analysis of the transcriptional regulation of the *Il17a* gene promoter [5–10]. Commitment to the Th17 lineage is dependent on T cell receptor signaling and requires IL-6- and TGFβ-induced signaling cascades [11]. In addition, IL-1β has been shown to be important and can substitute for TGFβ during early Th17 differentiation [12,13]. Several distinct components of the TCR signaling cascade have been specifically linked to CD4+ Th17 subset differentiation, such as the AP-1 transcription factor family member B cell-activating transcription factor (Batf), the Rel/NF-κB member c-Rel, Ikappaζ (IκBζ) and the Tec family tyrosine kinase member inducible T cell kinase (Itk) [5,8,9,14]. Itk specifically regulates NFATc1 binding to the *Il17a* promoter and activates the transcription of *Il17a* but not *Il17f*, *Il17a* appears to be the more pathogenic cytokine involved in the autoimmune response [9]. Several conserved noncoding sites (CNS) have been identified within the *Il17a–Il17f* locus, and the CNS2 region in particular has been associated with the permissive hyperacetylation of histone H3 [13–15]. Recently, it has been shown that the CNS2 region is and optimal *Il17f*

CD4+ Th17 differentiation is initiated by the subset-specific transcription factors retinoic acid-related orphan receptor (ROR)γt and RORα in combination with other transcription factors, such as the aryl hydrocarbon receptor (Ahr), the Runt-related transcription factor 1 (Runx1), interferon regulatory factor 4 (IRF4) and the signal transducer and activator of transcription 3 (STAT3). The coordinated activity of these factors subsequently induces the transcription of CD4+ Th17 cytokines including *Il17a*, *Il17f*, *Il21*, *Il22*, *Il23* and *Csf2r* [7,16–18].

The secretion of these proinflammatory cytokines by CD4+ Th17 cells must be tightly controlled to avoid tissue damage and autoimmune responses. Several negative regulators of CD4+ Th17 differentiation and function have been identified, including the transcription factors forkhead box protein P3 (Foxp3), signal transducer and activator of transcription 5 (STAT5), suppressor of cytokine signaling 3 (SOCS3), eomesodermin, growth factor-independent 1 (Gfi1), v-ets erythroblastosis virus E26 oncogene

* Corresponding authors. Tel.: +43 (0)512 9003 70514/70517; fax: +43 (0)512 9003 73510.
E-mail addresses: natascha.kleiter@i-med.ac.at (N. Hermann-Kleiter), Gottfried.baier@i-med.ac.at (G. Baier).

0896-8411
http://dx.doi.org/10.1016/j.jaut.2012.07.007

homolog 1 (Ets1), T-box transcription factor (T-bet) and inhibitor of DNA binding 3 (Id3) [16,19–26].

There is also emerging evidence for biologically important roles of nuclear receptor signaling in the regulation of Th17 subset differentiation and function [27]. Members of the nuclear receptor family regulate the CD4$^+$ Th17 T cell response with reciprocal outcomes; the RAR-related orphan receptors (RORγ/NR1F3 and RORα/NR1F3-A) are key transcriptional activators, whereas retinoic acid receptor (RAR/NR1B1), retinoid X receptor (RXR/NR2B1), nuclear receptor subfamily 2 group F member 6 (Ear2/NR2F6), peroxisome proliferator-activated receptor gamma (PPARγ/NR1C3), liver X receptor (LXR/NR1H), glucocorticoid receptor (GR/NR3C1), the vitamin D receptor (VDR/NR1I1) and the estrogen receptor (ER NR3A1) contribute anti-inflammatory effects [16,18,28–30].

We have previously demonstrated that the nuclear orphan receptor NR2F6 potently antagonizes the ability of Th17 CD4$^+$ T cells to induce the expression of *Il17a* in an NFAT-specific fashion [18]. As the precise mode of *Il17a* transcriptional regulation via NR2F6 has remained unclear, we investigated in detail how, where and in what context NR2F6 attenuates the DNA accessibility of NFAT and RORγt. We identified a crucial role for NR2F6 in the direct binding to multiple sites within the locus encoding *Il17a*. The subsequent suppression of *Il17a* transcription by NR2F6 represents an important physiological mechanism controlling Th17 cell effector functions.

2. Material and methods

2.1. Mice

Nr2f6-deficient mice [18] between the ages of 6–12 weeks were used for the experiments. *Nr2f6-Tg85* transgenic mice were generated by pronuclear injection (C57Bl/6 mouse eggs) of linearized and purified CAG-mNr2f6-2A-EGFP DNA. Transgenic mice were selected by PCR analysis of tail DNA with TaqMan probes for EGFP (probes from ABI) and were maintained on the C57/Bl6 background. The experimental protocols and animal care and handling methods conformed to the Swiss federal law for animal protection. The studies described in this report were performed according to the Novartis animal license numbers 1022 and 1331. B6.129P2(Cg)-Rorc^{tm2Litt}/J mice of 8–12 weeks of age were obtained from the Jackson laboratory. OTII mice obtained from Charles River Laboratories were crossed onto the *Nr2f6*-deficient C757Bl6 background. The mice were maintained under specific pathogen-free (SPF) conditions, and all animal experiments were performed in accordance with the Austria "Tierversuchsgesetz" (BGBI. Nr. 501/1988 i.d.g.F.) and have been granted by the Bundesministerium für Bildung, Wissenschaft und Kultur (bm:bwk).

2.2. MOG_{35-55}-induced EAE

Female mice were injected subcutaneously at the tail base with 200 μg MOG_{35-55} peptide (100 μl) (PolyPeptide group, France) in complete Freund's adjuvant (CFA) containing 5 mg/ml H37RA (Mycobacterium tuberculosis, Difco Laboratories, Detroit, Michigan, USA). Additionally, 200 ng pertussis toxin (Sigma Aldrich) was injected i.p. on days 0 and 2 post-CFA injection [18]. EAE disease severity was scored according to the previously described 0–4 scale [31] as follows: 0, no clinical signs; 0.5, tail weakness; 1, completely limp tail; 1.5, limp tail and hindlimb weakness; 2, unilateral hindlimb paralysis; 2.5, bilateral partial hindlimb paralysis; 3, bilateral hindlimb paralysis; 3.5, complete hindlimb and unilateral forelimb paralysis; and 4, death or moribund.

2.3. Adoptive EAE

Adoptive EAE was performed according to Miller [32] and Axtell [33]. Briefly, 8–10 days after immunization, the splenic and draining lymph node cells from MOG_{35-55} peptide-immunized *Nr2f6*$^{+/+}$ or *Nr2f6*$^{-/-}$ mice were isolated and depleted of red blood cells with lysis buffer (R&D Systems). The cells were re-stimulated with 25 μg/ml MOG_{35-55} (3×10^6/ml in IMDM) in the presence of 25 ng IL-23. After 5 days in culture, the cells were harvested, and 2×10^7 cells were transferred into healthy *Nr2f6*$^{+/+}$ recipients via i.p. injection. Pertussis toxin (200 ng/mouse; Sigma) was administered i.p. on the day of the adoptive transfer as well as 48 h after transfer. Signs of EAE disease were scored using a 0–4 scale, according to the methods of Hirota [13]. The frequencies of donor CD4$^+$ T cells producing IL-17 and IFNγ were assessed by FACS prior to transfer.

2.4. Preparation of mononuclear infiltrating cells

Mononuclear infiltrating cells were isolated from the CNS and SC as described by Korn and Hermann-Kleiter [18,34]. Briefly, the mice were perfused through the left cardiac ventricle, and the brain and SC were removed and flushed with PBS. The tissues were then digested with collagenase D (2.5 mg/ml; Roche Diagnostics) and DNaseI (1 mg/ml; Sigma) at 37 °C for 45 min. The homogenate was passed through a 70-μm cell strainer, and the mononuclear cells were isolated by Percoll density centrifugation (70%–30%). The cells were removed from the interphase, washed, and resuspended in IMDM complete medium (10% FCS, 2 mM L-Glutamine and 50 U ml^{-1} penicillin/streptomycin).

2.5. In vitro Th differentiation

Naive CD4$^+$ T cells were isolated using the CD4$^+$ CD62L$^+$ T cell isolation kit II (Miltenyi Biotech). Polarization of these CD4$^+$ T cells into Th17 cells was performed in complete IMDM medium supplemented with TGFβ (5 ng/ml), IL-6 (20 ng/ml), IL-23 (10 ng/ml), anti-IFNγ, and anti-IL-4 (2 μg/ml). The polarization of CD4$^+$ T cells into iTregs was performed in complete IMDM medium supplemented with TGFβ (5 ng/ml) plus hIL-2 (25 ng/ml).

2.6. Gel mobility-shift assay

Naive resting and Th1- and Th17-differentiated CD4$^+$ T cells were lysed, and nuclear extracts were prepared [18]. The following oligonucleotides were used, and the core binding motifs are underlined:

min. h*Il17a* (NFAT o3) [35] 5′-CATTGGGGGCGGAAATTTTAACCAA-3′;

min. *Il17a* (NFAT o3) mouse 5′-CATTTGAGGATGGAATCTTTACTCAAA-3′ and mutated.

Il17a (NFAT mo3) 5′-CATT*AAG*GGATGGAATCTTTACTCAAA-3′.

NFAT *Il17a* CNS2 5′-TTGGTTGGAAAAAAAAATGGAAAGTTTTCTGACCCACTTT-3′

RORE *Il17a* CNS2 [16] 5′-GAAAGTTTTCTGACCCACTTTAAATCAATTT-3′.

NR2F6-specific EMSAs were performed using the probe set for the COUP-TF family member NR2F1 (Panomics). This probe contains the same core binding sequence as NR2F6, as underlined (5′-GTGTCAAAGGTCGTGTCAAAGGTC-3′). Antibodies targeting NR2F6 (R&D PP-N2025-00), NFATc1 (ABR ma3-024), and RORγ(t) (eBioscience 14-6981) were used for the supershift experiments.

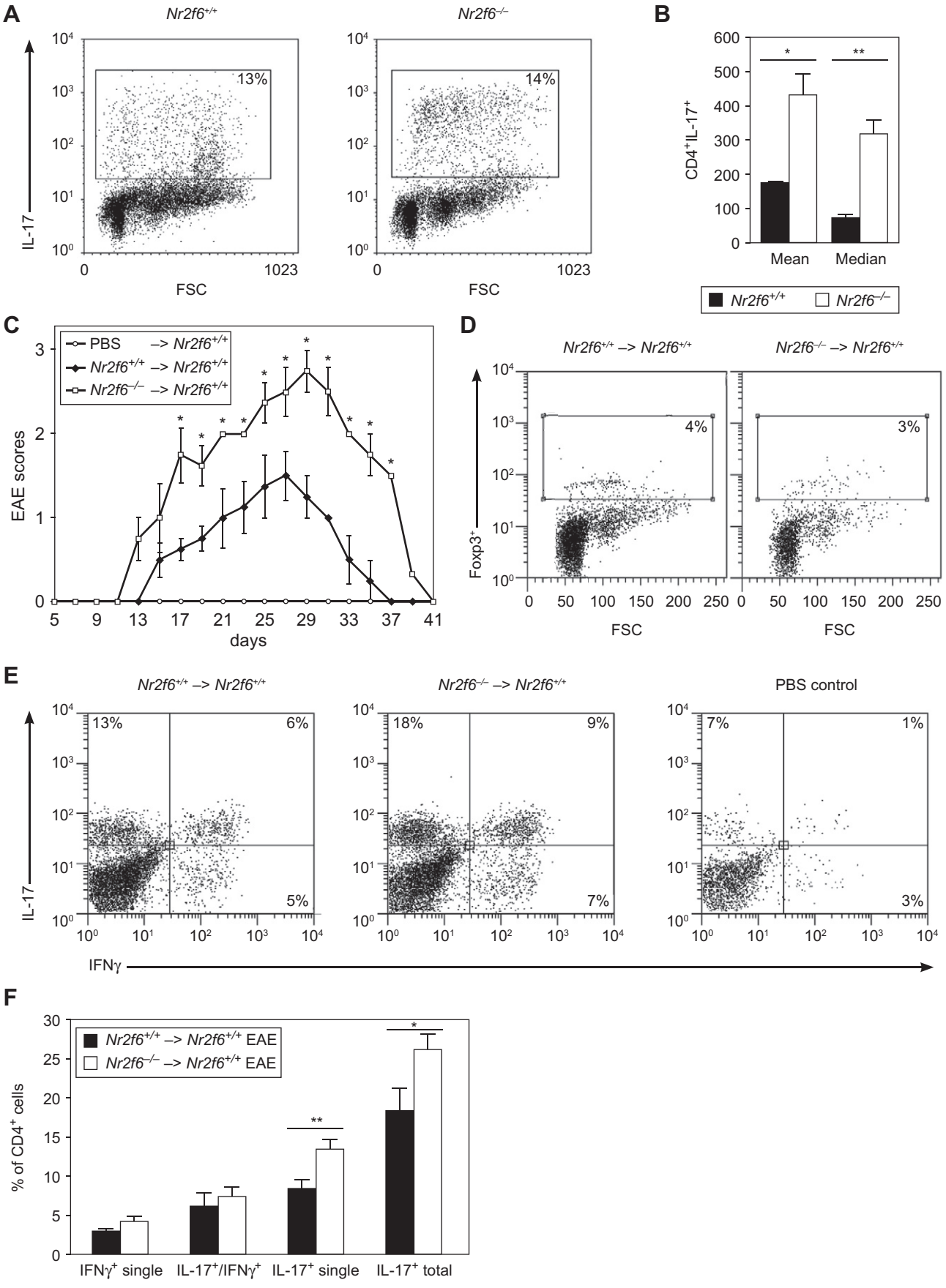
A
Nr2f6+/+
Nr2f6−/−
IL-17
FSC
13%
14%
B
CD4+IL-17+
Mean
Median
Nr2f6+/+
Nr2f6−/−
C
PBS –> Nr2f6+/+
Nr2f6+/+ –> Nr2f6+/+
Nr2f6−/− –> Nr2f6+/+
EAE scores
days
D
Nr2f6+/+ –> Nr2f6+/+
Nr2f6−/− –> Nr2f6+/+
Foxp3+
FSC
4%
3%
E
Nr2f6+/+ –> Nr2f6+/+
Nr2f6−/− –> Nr2f6+/+
PBS control
IL-17
IFNγ
13%
6%
5%
18%
9%
7%
7%
1%
3%
F
Nr2f6+/+ –> Nr2f6+/+ EAE
Nr2f6−/− –> Nr2f6+/+ EAE
% of CD4+ cells
IFNγ+ single
IL-17+/IFNγ+
IL-17+ single
IL-17+ total

2.7. ChIP

The chromatin immunoprecipitation (ChIP) assay was performed with a ChIP assay kit according to the recommendations of the manufacturer (Imgenex) in combination with the Cold Spring Harbor protocol [36]. Briefly, *Nr2f6*$^{+/+}$ and *Nr2f6*-deficient naïve T cells were isolated using the CD4$^+$ CD62L$^+$ T cell isolation kit II (Miltenyi Biotech). The polarization of CD4$^+$ T cells into Th17 cells was performed using solid-phase anti-CD3 (5 μg/ml) and soluble anti-CD28 (1 μg/ml) in complete IMDM medium supplemented with TGFβ (5 ng/ml), IL-6 (20 ng/ml), IL-23 (10 ng/ml), anti-IFNγ, and anti-IL-4 (2 μg/ml). The cells were harvested and washed once in IMDM on day 3 and re-stimulated overnight by solid-phase anti-CD3 (5 μg/ml) in IMDM medium. The Th17 cells were fixed in 1% formaldehyde at 37 °C for 10 min, and the cross-linking was quenched by the addition of 1.375 M glycine. The cells were then washed twice with ice-cold PBS and lysed in cold cell lysis buffer for ChIP (5 mM PIPES (pH 8.0), 85 mM KCl, 0.5% Nonidet P-40 (NP-40)) for 10 min. The cell pellets were lysed following centrifugation in 1 ml nuclei lysis buffer for ChIP (50 mM Tris-Cl (pH 8.0), 10 mM EDTA, 1% SDS) supplemented with protease inhibitors and were incubated for 10 min on ice. Following sonication with 25–30 s pulses using a Bioruptor Next Generation (Diagenode), the samples were centrifuged for 10 min at 12.000 rpm. The sheared chromatin was used to setup immunoprecipitation reactions with 5 μg of the indicated Abs (IgG sc-2027 Santa Cruz; NFATc1 sc-7294, RORyt sc-28559; H3K4 ab8580 Abcam, NR2F6 R&D PP-N2025-00) at 4 °C overnight. Magna ChIP protein G magnetic beads were added for 2 h, and the samples were sequentially washed once with the buffers provided by the supplier (IMGENEX; high to low salt). The DNA-protein complex was eluted by heating at 65 °C overnight, and the DNA was eluted using the IPure kit (Diagenode). Real-time PCR was performed with the following primers and probes using an ABI PRIM 7000 Sequence Detection System (Applied Biosystems):

Il17a minimal promoter (−243 to −176) 5′-GAACTTCTGCCCTTCCCATCT-3′ and 5′-CAGCACAGAACCACCCCTTT-3′ with the probe.

5′-FAM-CCTTCGAGACAGATGTTGCCCGTCA-TAMRA-3′ [8]; and *Il17a* CNS2 5′-CCGTTTAGACTTGAAACCCAGTC-3′ and 5′-GTACC-TATGTGTTAGGAGGCGC-3′, with the probe 5′-FAM-CAAGTGGGGGC-CATCAGTC-TAMRA-3′ [16].

2.8. Flow cytometry

Cells were either unstimulated or stimulated with PMA/ionomycin (50 ng/ml; 500 ng/ml) for 5 h in the presence of Golgi stop (BD Bioscience). The expression of CD4, IL-17, IL-17A, IFNγ (BD Pharmingen), RORγt, and Foxp3 (eBioscience) was analyzed by intracellular staining (Cytofix/Cytoperm kit plus, BD Biosciences or eBioscience buffer) followed by FACS analysis (FACSCalibur, BD Biosciences).

2.9. Gene expression analysis

Total RNA was isolated using the Qiagen RNeasy kit. The first-strand cDNA synthesis was performed using oligo(dT) primers (Promega) with the Qiagen Omniscript RT kit, according to the instructions of the supplier. The expression analysis was performed using real-time PCR with an ABI PRIM 7000 Sequence Detection System (Applied Biosystems) with TaqMan gene expression assays, and all expression patterns were normalized to that of *Gapdh*. The expression levels of wildtype Th17-stimulated cells were arbitrarily set to 100.

Table 1
Transfer of MOG_{35-55}-specific Th17 cells into wild-type recipients.

Genotype	Incident	Onset day (mean ± s.e.m)	Max. score (mean ± s.e.m)
Control	0% (0/1)	NA	NA
Nr2f6$^{+/+}$	100% (4/4)	d15 ± 0.2	1.38 ± 0.38
Nr2f6$^{-/-}$	100% (4/4)	d13 ± 0.25	2.75 ± 0.25

2.10. Western blotting

Cells were stimulated for the indicated lengths of time, washed, and lysed in lysis buffer. Whole-cell extracts or nuclear extracts were electrophoresed on NuPAGE gels (Invitrogen) and transferred to PVDF membranes. Protein lysates were subjected to immunoblotting with antibodies against Rory (Santa Cruz sc-28559), ROR gamma (t) (eBioscience 14-6981), NFATc1 (Santa Cruz sc-7294), NFATc2 (Santa Cruz sc-7295x), HA (Covance MMs-101P) and DNA polymerase-δ (Santa Cruz sc-10784).

2.11. Co-immunoprecipitation

The co-immunoprecipitation analysis was described previously [37].

2.12. Statistical analysis

Differences between genotypes were analyzed using the unpaired Student's *t* test. Significant differences are indicated as follows: $^*p < 0.05$; $^{**}p < 0.01$; or $^{***}p < 0.001$.

3. Results

3.1. Immune cell-intrinsic NR2F6 is required to suppress EAE disease progression

Nr2f6-deficient mice are more susceptible to the induction of experimental autoimmune encephalomyelitis (EAE) [18]. To exclude the possibility that the enhanced Th17 development and EAE disease progression in *Nr2f6*-deficient mice is caused by altered dendritic or microglial cells, we employed an adoptive EAE lymphocyte transfer model. Splenocytes and draining lymph node cells from MOG_{35-55}-immunized *Nr2f6*$^{+/+}$ or *Nr2f6*$^{-/-}$ mice were stimulated *ex vivo* with MOG_{35-55} in the presence of IL-23 for 5 days and were then injected into naïve *Nr2f6*$^{+/+}$ recipient mice. The percentage of differentiating CD4$^+$ IL-17$^+$-producing cells was determined by FACS analysis prior to transfer into the recipient animals. Despite comparable total CD4$^+$ IL-17$^+$ cell numbers, the *Nr2f6*$^{-/-}$ CD4$^+$ T cells demonstrated significantly increased IL-17 expression on a per-cell basis (Fig. 1 A and B).

Fig. 1. Immune cell-intrinsic NR2F6 is required to suppress EAE disease progression. (A) For adoptive EAE, the draining lymph node cells and splenocytes from MOG_{35-55}-immunized *Nr2f6*$^{+/+}$ or *Nr2f6*$^{-/-}$ mice were restimulated *in vitro* with MOG_{35-55} in the presence of IL-23 for 5 days and were then analyzed by flow cytometry for intracellular staining of IL-17A (CD4$^+$ gated events). (B) Quantification of the positively gated IL-17A CD4$^+$ cells is presented. Data are representative of two independent experiments with three mice per group. (C) EAE disease time course of naïve syngeneic *Nr2f6*$^{+/+}$ mice injected intraperitoneally with either (2×10^7) *Nr2f6*$^{+/+}$ or *Nr2f6*$^{-/-}$ *in vivo* EAE-primed and *in vitro* re-stimulated cells. (D) CD4$^+$ Foxp3$^+$ staining revealed no significant difference in CNS-infiltrating regulatory T cells between the experimental groups, as shown by one representative FACS dot blot of Foxp3$^+$ cells gated on CD4$^+$ T cells. Data are representative of two independent experiments with three mice per group. Error bars, mean ± s.e.m. $^*p < 0.05$. (E) Flow cytometry of mononuclear cells isolated from the brains of mice with adoptively transferred disease. The IL-17A- and IFNγ-positive cells were gated on CD4$^+$ cells; one representative example from the adoptive transfer of *Nr2f6*$^{+/+}$ or *Nr2f6*$^{-/-}$ cells or PBS into *Nr2f6*$^{+/+}$ mice is shown. (F) The quantification of the CD4-positively gated IL-17A and IFNγ cells infiltrating the CNS is shown. Data are representative of two independent experiments with three mice per group. Error bars, mean ± s.e.m. $^*p < 0.05$; $^{**}p < 0.01$.

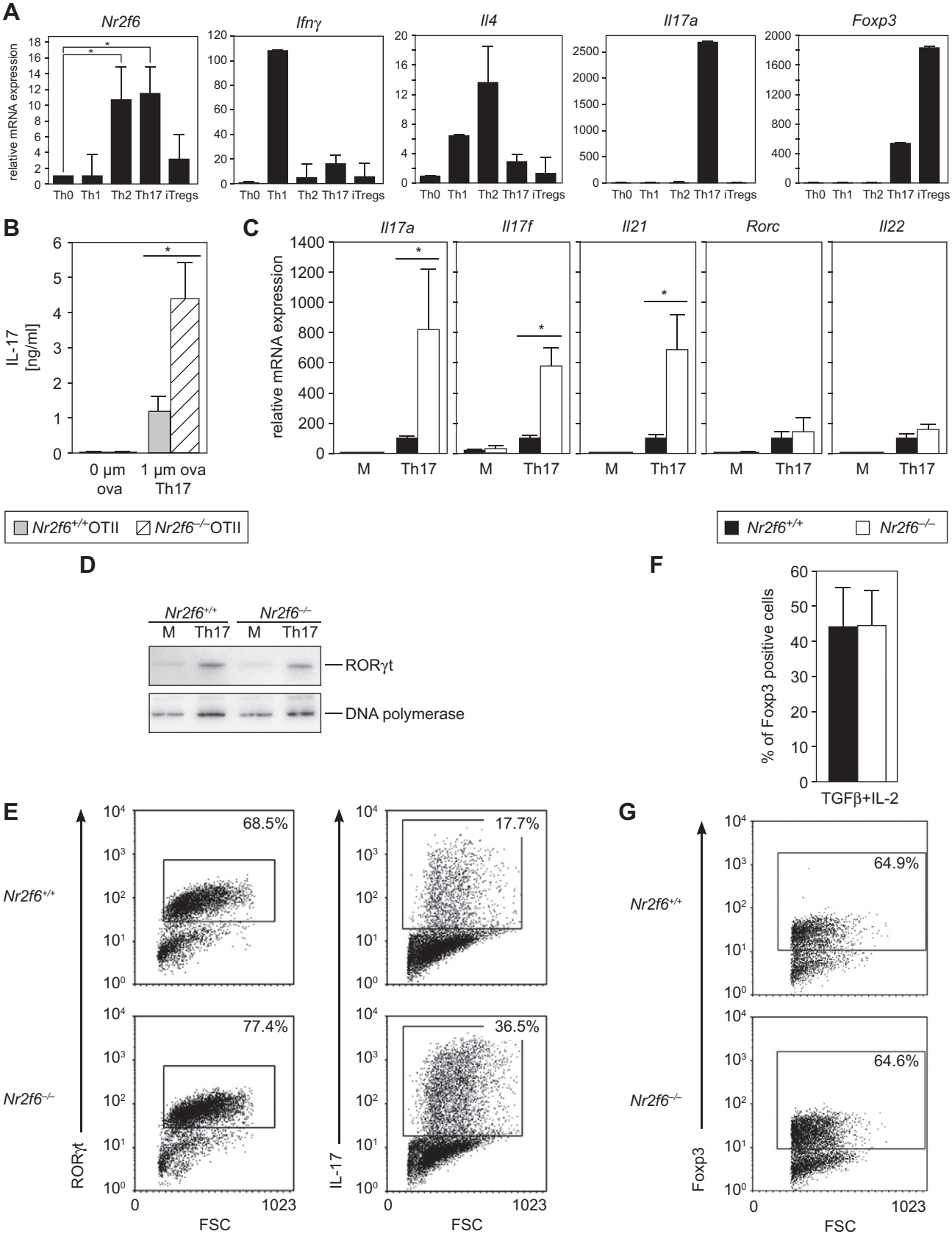

Fig. 2. *Nr2f6* is mainly expressed in the Th2 and Th17 subset and suppresses *Il17a*, *Il17f* and *Il21 transcription but not RORγt or iTreg induction*. (A) Naïve CD4$^+$ T cells were differentiated under neutral Th0, Th1, Th2, Th17 and iTreg conditions, and *Nr2f6* mRNA expression was assessed by qRT-PCR. The Th subset-polarizing conditions were controlled by mRNA expression of *Ifng* (Th1), *Il4* (Th2), *Il17a* (Th17) and Foxp3 (iTregs). The data shown are derived from at least three independent experiments demonstrating consistent results. qRT-data were normalized to *Gapdh* expression. Error bars denote the mean ± s.e.m. $^*p < 0.05$; expression in the Th0 subset was arbitrarily set to 1. (B) IL-17A secretion by OT-II

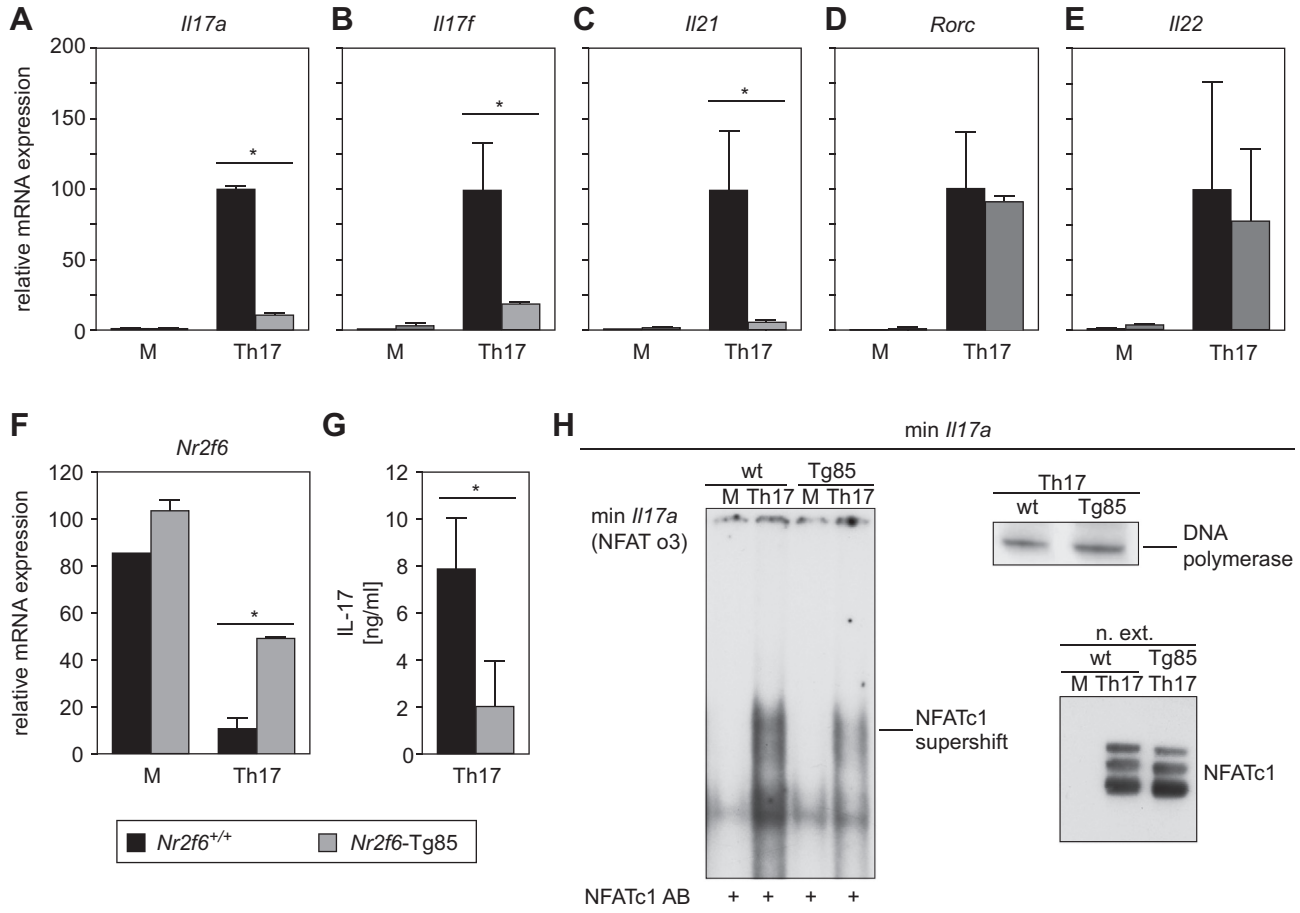

Fig. 3. *Nr2f6* overexpression suppresses Th17 differentiation *in vitro*. (A) Wildtype (*Nr2f6*$^{+/+}$) or *Nr2f6*-Tg85 (Tg85) CD4$^+$ cells were differentiated under Th17 conditions, and *Il17a*, (B) *Il17f*, (C) *Il21*, (D) *Rorc*, (E) and *Il22* transcript levels from both genotypes were determined by qRT-PCR. The data shown are derived from three independent experiments and are normalized to the amounts of *Gapdh* expression. Expression in the Th17 *Nr2f6*$^{+/+}$ differentiated cells subset was arbitrarily set to 100 in order to facilitate comparison between the different cytokines. Error bars denote the mean ± s.e.m. $^*p < 0.05$. The error bars denote mean ± s.e.m. $^*p < 0.05$. (F) Expression of *Nr2f6* in *Nr2f6*$^{+/+}$ or *Nr2f6*-Tg85 un-stimulated or Th17-differentiated CD4$^+$ T cells. Note the approximate 4-fold increase in expression in the Tg85 transgenic *NR2F6* cells. (G) Supernatants from wildtype (*Nr2f6*$^{+/+}$) or *Nr2f6*-Tg85 (Tg85) CD4$^+$ Th17-differentiated cells were used to measure IL-17 secretion via BioPlex. (H) EMSA analysis of nuclear extracts prepared from wildtype (*Nr2f6*$^{+/+}$) or Tg85 CD4$^+$ Th17-differentiated cells hybridized to the min *Il17a* (NFAT o3) oligonucleotide and supershifted with an NFATc1 antibody. Equal NFAT nuclear translocation was observed by western blot, and DNA polymerase δ was used as the loading control. One of three independent experiments is shown.

Naïve *Nr2f6*$^{+/+}$ mice treated with MOG_{35-55}-primed *Nr2f6*-deficient cells developed significantly more severe EAE disease without changing Foxp3 levels of infiltrating CD4$^+$ T cells (Fig. 1C and D and Table 1). Significantly higher levels of infiltrating CD4$^+$ IL-17$^+$ T cells were found in the central nervous system of mice that received MOG_{35-55}-primed *Nr2f6*$^{-/-}$ cells in comparison to recipients that received MOG_{35-55}-primed *Nr2f6*$^{+/+}$ cells (Fig. 1E and F).

3.2. Attenuation of Il17a, Il17f and Il21 gene transcription in *Nr2f6*$^{-/-}$ CD4$^+$ Th17 cells

We have previously shown that NR2F6 potently antagonizes the ability of CD4$^+$ Th17 cells to secrete the signature cytokine IL-17A following TCR stimulation under Th17-differentiating conditions [18]. To understand why NR2F6 is critical in CD4$^+$ Th17 T cells, we analyzed its expression in the different Th subsets. qRT-PCR of *Nr2f6*$^{+/+}$-differentiated CD4$^+$ Th0, Th1, Th2, Th17 and iTreg T cell subsets revealed that *Nr2f6* mRNA is predominately expressed in the Th17 and Th2 subsets but not the Th1 and iTreg subsets.

Specific Th subset differentiation was controlled by the expression patterns of key cytokines associated with Th1 (*Ifng*), Th2 (*Il4*) and Th17 (*Il17a*) cells as well as that of the Treg-specific transcription factor Foxp3 (Fig. 2A).

We next crossed *Nr2f6*-deficient mice to an OT-II TCR-transgenic background to investigate Th17 cell functions during physiological stimulation with cognate antigen. *Nr2f6*-deficient OT-II TCR-

Nr2f6$^{+/+}$ or OT-II *Nr2f6*$^{-/-}$ CD4$^+$ Th17 cells in the presence of unstimulated DCs or DCs pulses with 1 μm Ova for 3 d was measured in the supernatant via BioPlex method. The data shown are derived from three independent experiments. (C) Naïve *Nr2f6*$^{+/+}$ or *Nr2f6*$^{-/-}$ CD4$^+$ T cells were Th17- (TGFβ, IL-6, IL-23, αIL-4, αIFNγ) differentiated, and the expression of *Il17a*, *Il17f*, *Il21*, *Rorc* and *Il22* mRNA was assessed by qRT-PCR. The data shown are derived from at least three independent experiments demonstrating consistent results. qRT-data were normalized to *Gapdh* expression. Expression in the Th17 *Nr2f6*$^{+/+}$ differentiated cells subset was arbitrarily set to 100 in order to facilitate comparison between the different cytokines. Error bars denote the mean ± s.e.m. $^*p < 0.05$. (D) Western blot analysis of nuclear extracts from *Nr2f6*$^{+/+}$ or *Nr2f6*$^{-/-}$ CD4$^+$ Th17- (TGFb, IL-6, IL-23, αIL-4, αIFNg) differentiated cells revealed no differences in the amount of nuclear RORγt protein; DNA polymerase was used as a loading control. The data shown represent one of three independent experiments. (E) Flow cytometry of *in vitro* Th17- (TGFb, IL-6, IL-23, αIL-4, αIFNg) differentiated *Nr2f6*$^{+/+}$ or *Nr2f6*$^{-/-}$ CD4$^+$ Th17 cells. No significant difference in RORγt staining could be observed, although IL-17 staining was different between the two genotypes. One representative example of three is shown. (F) Quantification of the positively gated Foxp3$^+$ CD4$^+$ cells stimulated with TGFβ in combination with IL-2. Data represent a summary of three independent experiments. Error bars denote the mean ± s.e.m. (G) Flow cytometry of *in vitro*-differentiated (TGFβ$^+$ IL-2) *Nr2f6*$^{+/+}$ or *Nr2f6*$^{-/-}$ Foxp3-positive CD4$^+$ T cells; one representative example is shown.

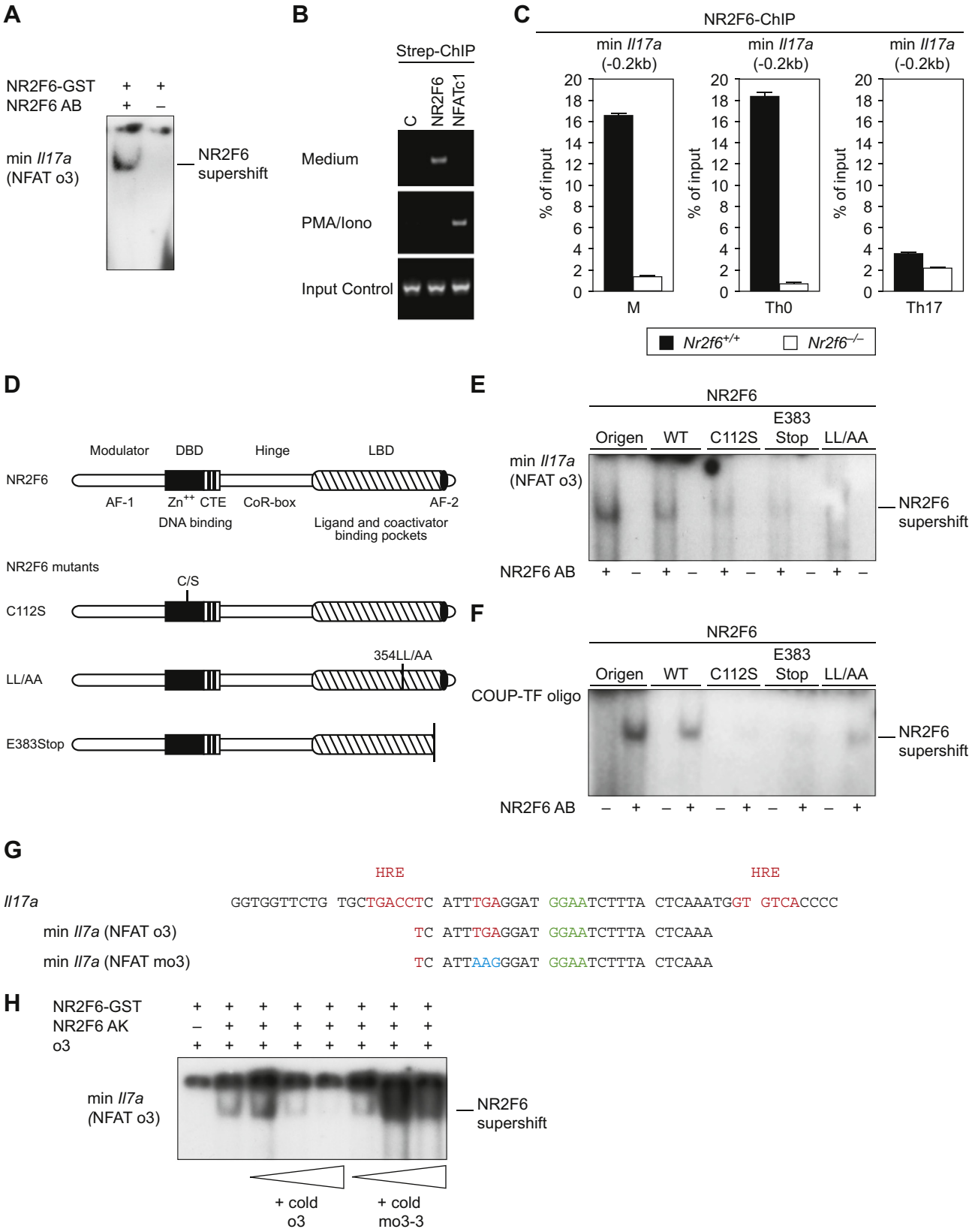

Fig. 4. Direct NR2F6 binding to the minimal *Il17a* promoter is dependent on its DNA- and ligand-binding domains. (A) GST-NR2F6 binds to min *Il17a* (NFAT o3) of the *Il17a* promoter region in electromobility shift assays. (B) Strep-ChIP assay in Jurkat cells transfected with NR2F6 or NFATc1 Strep-tagged proteins and the *Il17a* promoter region (1.3 kb). Jurkat cells were either rested (medium) or stimulated overnight (ON) with PMA/Iono, and the cell lysates were immunoprecipitated with an anti-Strep antibody and amplified with a primer pair for the minimal *Il17a* promoter. The data shown are derived from two independent experiments demonstrating consistent results. (C) ChIP analysis of naive *Nr2f6*$^{+/+}$ or *Nr2f6*$^{-/-}$ CD4^{+} T cells either left unstimulated or stimulated under Th0 or Th17 conditions for 3 days, then stimulated with αCD3 ON, crosslinked with formaldehyde and immunoprecipitated with anti-NR2F6. The bound DNA was amplified by qRT-PCR using a primer pair from the minimal *Il17a* promoter locus. (D) The schematic depicts a series of mutant NR2F6

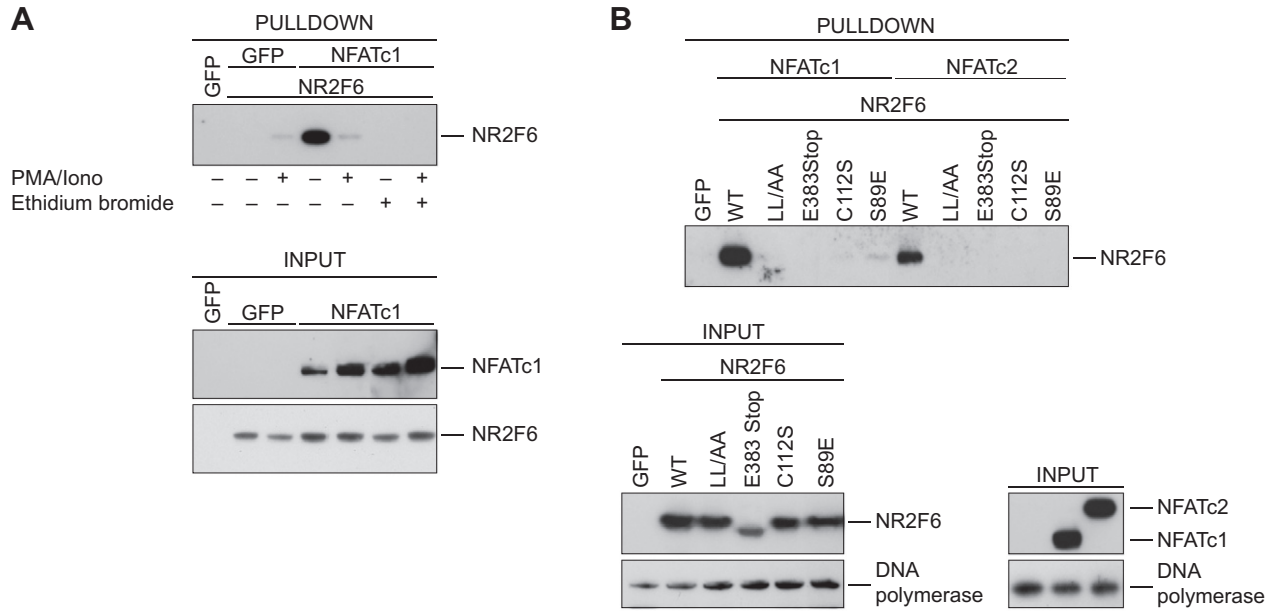

Fig. 5. Physical interaction between NR2F6 and NFATc1 is dependent on DBD and LBD domains of NR2F6. Unstimulated or PMA/Iono-stimulated Jurkat cells were cotransfected with wildtype and mutant NR2F6-His, Strep-HA tagged NFATc1 and the *Il17a* promoter region (1.3 kb) constructs, and nuclear protein extracts were pulled down with Streptavidin beads. (A) Anti-Strep immunoprecipitates of the total nuclear lysates were immunoblotted with anti-His and anti-HA antibodies, which revealed direct binding of NR2F6-NFATc1 in resting but not PMA/Iono-stimulated cells. The addition of ethidium bromide destroyed the interaction between NR2F6 and NFATc1 in resting cells. (B) DNA (C112S; S89E) and ligand binding domain (LL/AA: E383Stop) mutants of NR2F6 lost their affinity to bind NFATc1 or NFATc2 in resting Jurkat cells, in contrast to wt-NR2F6. The input and GFP-negative controls are shown, along with the DNA polymerase loading control. One of three independent experiments is shown.

transgenic Th17 CD4$^+$ T cells again exhibited significantly greater IL-17A secretion (Fig. 2B) but manifested comparable levels of RORγt expression (data not shown).

Next, we performed a more detailed expression profile analysis of *Il17a*, *Il17f*, *Il21* and *Il22*, as well as the key transcription factor *Rorc*, during Th17 differentiation. When naïve *Nr2f6*$^{+/+}$ or *Nr2f6*-deficient CD4$^+$ T cells were activated under Th17 differentiation conditions (TGFβ, IL-6, IL-23, αIL-4, αIFNγ), the expression levels of *Il17a* and *Il17f*, as well as *Il21*, were significantly higher in the *Nr2f6*-deficient CD4$^+$ Th17 cells. The *Rorc* and *Il22* expression levels were not significantly altered (Fig. 2C), indicating that NR2F6-mediated regulation of the *Il17a*, *Il17f* and *Il21* promoters is context-dependent. RORγt protein levels were also analyzed by western blot and intracellular FACS analysis, and again no significant differences were observed in *Nr2f6*-deficient CD4$^+$ Th17 cells despite a slight increase in the intracellular FACS analysis (Fig. 2D and E).

Exposure of naïve CD4$^+$ T cells to TGFβ in the presence of IL-6 triggers Th17 differentiation, whereas the presence of IL-2 favors differentiation into Foxp3-expressing iTregs. We therefore investigated the potential for naïve *Nr2f6*-deficient CD4$^+$ T cells to differentiate into Foxp3-expressing iTregs. The differentiation of *Nr2f6*$^{+/+}$ or *Nr2f6*-deficient naïve CD4$^+$ T cells with TGFβ plus IL-2 resulted in equivalent numbers of Foxp3$^+$ CD4$^+$ T cells, which suggests that NR2F6 does not play an essential role in the differentiation of iTregs (Fig. 2F and G). In support of this finding, the *Nr2f6*-deficient Treg suppressive functions were not significantly altered (data not shown).

3.3. Forced overexpression of NR2F6 suppresses Th17 cell function

To further validate the negative regulatory function of NR2F6, we generated a transgenic mouse line overexpressing NR2F6. *Nr2f6*-Tg85 mice exhibited severely suppressed CD4$^+$ Th17 cell functions, as measured by IL-17A secretion and *Il17a*, *Il17f* and *Il21* expression levels (Fig. 3A–C). Similar to the *Nr2f6*$^{-/-}$ cells, *Rorc and Il22* were not significantly different from wildtype levels (Fig. 3D–E). The qRT-PCR results revealed an approximate four-fold increase in *Nr2f6* expression in *Nr2f6*-Tg85 CD4$^+$ cells during Th17 differentiation as compared to wildtype cells (Fig. 3F and G).

We have previously shown that NFAT binding to a specific minimal *Il17a* promoter oligonucleotide (hereafter referred to as "min *Il17a* NFAT o3") is enhanced in *Nr2f6*-deficient *in vitro*-differentiated CD4$^+$ Th17 cells [18]. Therefore, we analyzed NFAT binding behavior using the nuclear extracts of Tg85-*NR2F6* CD4$^+$ Th17-differentiated cells and found reduced NFAT binding in cells of the transgenic line, although the nuclear translocation of NFAT was not altered (Fig. 3H).

3.4. NR2F6 binds directly to the minimal Il17a promoter

To understand the mode of *Il17a* repression by NR2F6 in further detail, we determined whether recombinant NR2F6-GST could bind to the *Il17a* promoter sequence *in vitro*. Despite the lack of a consensus idealized hormone response element (HRE) half site containing a TGACCG motif, NR2F6-GST binding to the minimal

proteins with either a defective DNA binding domain (C112S; S89E) or ligand-binding domain (LL/AA; E383Stop). (E) *In vitro*-derived NR2F6 (from Origen) and NR2F6-GST but not the DNA (NR2F6-C112S) and ligand-binding domain mutants (NR2F6 E383Stop; LL/AA) bound to the min *Il17a* (NFAT o3) in EMSAs (F) a COUP-TF oligonucleotide was used as the positive control. The binding of NR2F6 is dependent on the presence of a supershift NR2F6 antibody. One of three independent experiments is shown. (G) Sequence of the mouse *Il17a* promoter region containing the min *Il17a* (NFAT o3) (underlined) (NFAT core sequence is highlighted in green), as well as the two HREs (confirmed for RORγt [46];) and the core motif of the second half site of the NR2F6 binding sites (highlighted in red), are shown. min *Il17a* (NFAT o3): 5′-CCTC ATTTGAGGAT GGAATCTTTA CTCAAA -3′; min *Il17a* (NFAT mo3): 5′-CCTC ATT**AAG**GGAT GGAATCTTTA CTCAAA -3′. (H) EMSA analysis revealed that binding of NR2F6 was only disturbed when using min. *Il17a* (NFAT mo3), suggesting that this TGA represents a NR2F6 *in vivo* binding half site. NR2F6 can also bind to the RORE sites [46] within the min. *Il17a* promoter. One of two independent experiments is shown.

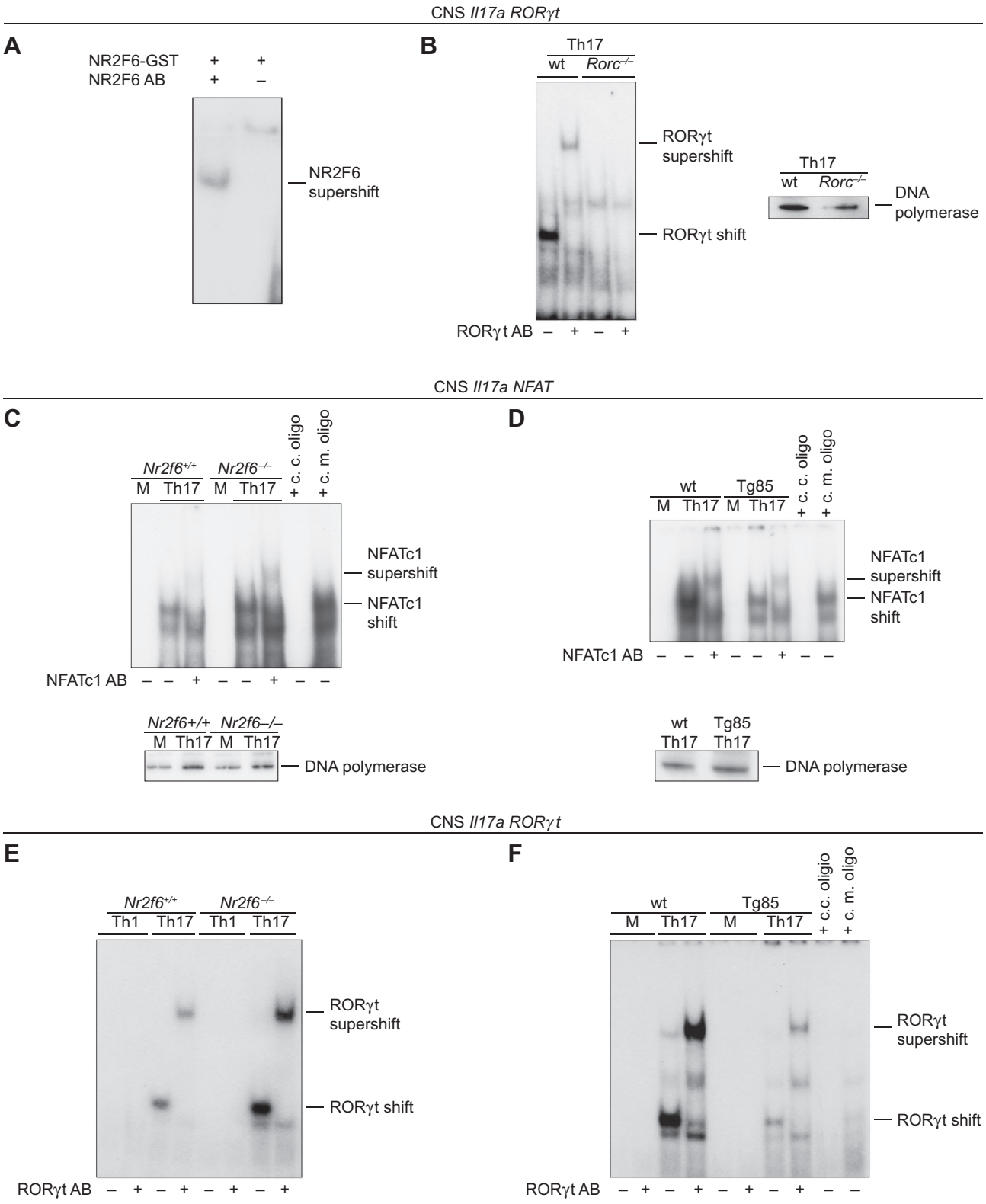

Fig. 6. NR2F6 suppresses NFAT and RORγt binding to the CNS2 region of the *Il17a* promoter. (A) GST-NR2F6 binds to the CNS2 *Il17a* RORγt oligonucleotide [16] of the *Il17a* CNS2 promoter region in EMSA analysis. (B) EMSA analysis of nuclear extracts from wildtype (wt) or Rorc$^{-/-}$ CD4^{+} T cells stimulated under Th17 conditions for 3 days and hybridized to the CNS2 *Il17a* ROR oligonucleotide. The specific binding of RORγt was confirmed using a RORγt supershift antibody loading was controlled by performing western blots with nuclear extracts probed with DNA polymerase δ no gross differences could be observed between the genotypes within the same stimulation conditions. (C) EMSA analysis of nuclear extracts of *Nr2f6*$^{+/+}$ or *Nr2f6*$^{-/-}$ CD4^{+} T cells either left unstimulated (M) or stimulated under Th17 conditions for 3 days and hybridized to a CNS2 *Il17a* NFAT-specific oligonucleotide. (D) EMSA analysis of nuclear extracts of wildtype (*Nr2f6*$^{+/+}$) or *Nr2f6*-Tg85 CD4^{+} T cells stimulated under Th17 conditions for 3 days and hybridized to a CNS2 *IL17a* NFAT-specific oligonucleotide. The specific binding of NFATc1 was confirmed using the NFATc1 supershift antibody and cold (c.c. oligo) and mutant competition oligonucleotides (c.m. oligo). (E) EMSA analysis of nuclear extracts from *Nr2f6*$^{+/+}$ or *Nr2f6*$^{-/-}$ CD4^{+} T cells stimulated under Th1 or under Th17 conditions for 3 days and hybridized to the CNS2 *Il17a* RORγ oligonucleotide. (F) EMSA analysis of nuclear extracts from wildtype (*Nr2f6*$^{+/+}$) or *Nr2f6*-Tg85 CD4^{+} T cells stimulated under Th17 conditions for 3 days and hybridized to the CNS2

Il17a NFAT o3 promoter oligonucleotide could be observed in electromobility shift assays (EMSA) *in vitro* (Fig. 4A).

Next, we performed chromatin immunoprecipitation (ChIP) assays with recombinant Strep-epitope-tagged NR2F6 and NFAT from transiently transfected Jurkat cells. Whereas recombinant NR2F6 bound to the minimal *Il17a* promoter under resting conditions, recombinant NFAT did not. When the Jurkat cells were stimulated with PMA/Iono, recombinant NR2F6 binding diminished, whereas recombinant NFAT binding was induced (Fig. 4B). In primary $CD4^+$ cells, we detected NR2F6 binding within the minimal *Il17a* promoter region in resting and *in vitro*-generated Th0 cells, whereas this binding was lost in Th17 differentiated cells. Moreover, no relevant binding could be observed in the *Nr2f6*-deficient cells used as negative controls for confirming the specificity of the NR2F6-ChIP antibody (Fig. 4C).

Using different mutant recombinant proteins for the DNA binding domain (DBD) and the ligand-binding domain (LBD), we determined the NR2F6 domains that are important for DNA binding (Fig. 4D). *In vitro*, proper binding to the minimal *Il17a* NFAT o3 promoter oligonucleotide was dependent on both the LBD and DBD of NR2F6 and occurred only in the presence of the NR2F6 antibody, indicating dependency on a homodimerization partner (Fig. 4E). When a chicken ovalbumin upstream promoter transcription factor (COUP-TF)-specific oligonucleotide sequence containing two HRE half sites was used as a positive control, NR2F6-GST binding again was dependent on the presence of both an intact DBD and LBD (Fig. 4F). To define the direct binding sequence of NR2F6, we performed mutational analysis and used competitor DNA oligonucleotide sequences. These experiments revealed the presence of a bona-fide half site within the minimal *Il17a* promoter directly 4 base pairs upstream of the NFAT core binding sequence of the minimal *Il17a* NFAT o3 promoter oligonucleotide (Fig. 4G and H).

3.5. NR2F6 directly interacts with NFAT in a DNA scaffold-dependent way

To understand how NR2F6 inhibits NFAT binding to the *Il17a* promoter, we co-expressed NR2F6 with HA-Strep-epitope-tagged NFATc1 or NFATc2 together with a plasmid encoding the *Il17a* promoter (1.3 kb) in Jurkat cells. Pull-down assays revealed that NR2F6 could physically interact with both NFATc1 and NFATc2 in resting Jurkat cells, and this association was dependent on the presence of DNA, as ethidium bromide disrupted this physical interaction (Fig. 5A). Of note, NR2F6 did not bind to RORγt in the same experimental setup (data not shown). Additionally, NR2F6 could only physically interact with NFATc1/c2 if the DBD and LBD domains were intact, as demonstrated using DNA (C112S; S89E) and ligand binding (LL/AA: E383Stop) domain-mutant recombinant proteins, confirming the DNA-dependent association of this protein complex (Fig. 5B). This finding suggests that NFATc1 and NFATc2 are the direct physical targets of DNA-bound NR2F6 in resting T cells.

3.6. NR2F6 suppresses NFAT and RORγt binding to the CNS2 Il17a promoter region

The *Il17a* CNS2 region contains HREs that have been shown to bind RORα and RORγt, which both strongly enhance the transcription of *Il17a* [16]. The HREs of the nuclear receptor family are highly homologous; therefore, we hypothesized that NR2F6 may be capable of binding this region as well. The capacity of recombinant NR2F6 to bind to this sequence was tested via EMSA. In fact, NR2F6-GST was able to directly bind to the oligonucleotide containing the HRE within CNS2, hereafter referred to as "CNS2 *Il17a* RORγt", *in vitro* (Fig. 6A) (previously published by Yang [16]). The specificity of this oligonucleotide was further verified using *Rorc*-deficient $CD4^+$ Th17 cells as a negative control (Fig. 6B).

We next analyzed the capacity of NFAT to bind to the CNS2 region in *Nr2f6*-deficient $CD4^+$ Th17 nuclear extracts and found that binding was enhanced in nuclear extracts derived from *Nr2f6*-deficient cells, compared to wildtype cells, using a CNS2 *Il17a* NFAT oligonucleotide (Fig. 6C). The NFAT binding capacity at the CNS2 locus was also analyzed in *Nr2f6*-Tg85 Th17 nuclear extracts, and reduced binding was consistently observed in *Nr2f6*-Tg85 $CD4^+$ Th17-differentiated nuclear extracts (Fig. 6D). The NFAT binding capacity for a specific Itk-dependent NFAT site at −3085 bp of the *Il17a*-proximal region [9] which is not flanked by an HRE, was not altered in *Nr2f6*-deficient Th17 cells (data not shown).

Thus, we hypothesized that RORγt binding may be altered in *Nr2f6*-deficient $CD4^+$ Th17 cells because both of these nuclear receptors can bind to the same HREs. In fact, an EMSA analysis using the CNS2 *Il17a* RORγt oligonucleotide probe revealed enhanced RORγt binding in *Nr2f6*-deficient $CD4^+$ Th17 nuclear extracts but no binding in Th1-derived nuclear extracts (Fig. 6E). Reduced RORγt binding was observed in nuclear extracts from *Nr2f6*-Tg85 $CD4^+$ Th17-differentiated cells (Fig. 6F).

3.7. Loss of Nr2f6 enhances NFAT and RORγt binding capabilities at the CNS2 and minimal Il17a promoter regions

To validate the EMSA results through an independent approach, we also performed ChIP analysis using NFAT, RORγt, H3K4 and IgG antibodies and two different primer pairs spanning the minimal and CNS2 regions of the *Il17a* promoter [7,8]. Wild-type and Nr2f6-deficient naïve $CD4^+$ cells were differentiated into Th0 and Th17 subsets for 3 days and subsequently re-stimulated overnight with αCD3. Significantly enhanced binding of NFATc1 and RORγt to both the CNS2 and minimal *Il17a* promoter regions was detected in *Nr2f6*-deficient $CD4^+$ Th17 cells. These data strongly suggest that NR2F6 inhibits the promoter activity of *Il17a* not only by suppressing NFAT but also by antagonizing RORγt binding (Fig. 7). The proposed regulation of *Il17a* transcription by NR2F6 is summarized in Fig. 8.

4. Discussion

How Th17 cell-mediated *Il17a* promoter activation is initiated and maintained is an area of active research. Here, we demonstrated that the nuclear orphan receptor NR2F6 can directly bind to the *Il17a* locus and interfere with the DNA-binding capacity of NFAT at the *Il17a* minimal promoter and CNS2 region. NFAT has been shown to play a critical role in the activation of the *Il17a* locus, as well as in EAE disease progression, through its binding to the *Il17a* promoter, and these findings have also been confirmed for the minimal promoter and several CNS regions [6,9,35,38].

In *Nr2f6*-deficient Th17 $CD4^+$ T cells, NFAT binding to the *Il17a*-*Il17f* locus was not increased overall but was specifically enhanced at sites flanked by an HRE, indicating that the trans-repression of NFAT by NR2F6 is dependent on the close proximity of these two sites.

Il17a RORγ oligonucleotide. The specific binding of RORγt was confirmed using a RORγt supershift antibody as well as a cold (c.c. oligo) and mutant competition oligonucleotide (c.m. oligo). Unspecific binding of the RORc oligonucleotide was validated via comparison with $Rorc^{-/-}$ $CD4^+$ Th17 cells (B). Equal loading was confirmed by performing western blots for nuclear extracts probed with DNA polymerase δ. The data shown are derived from at least three independent experiments demonstrating consistent results.

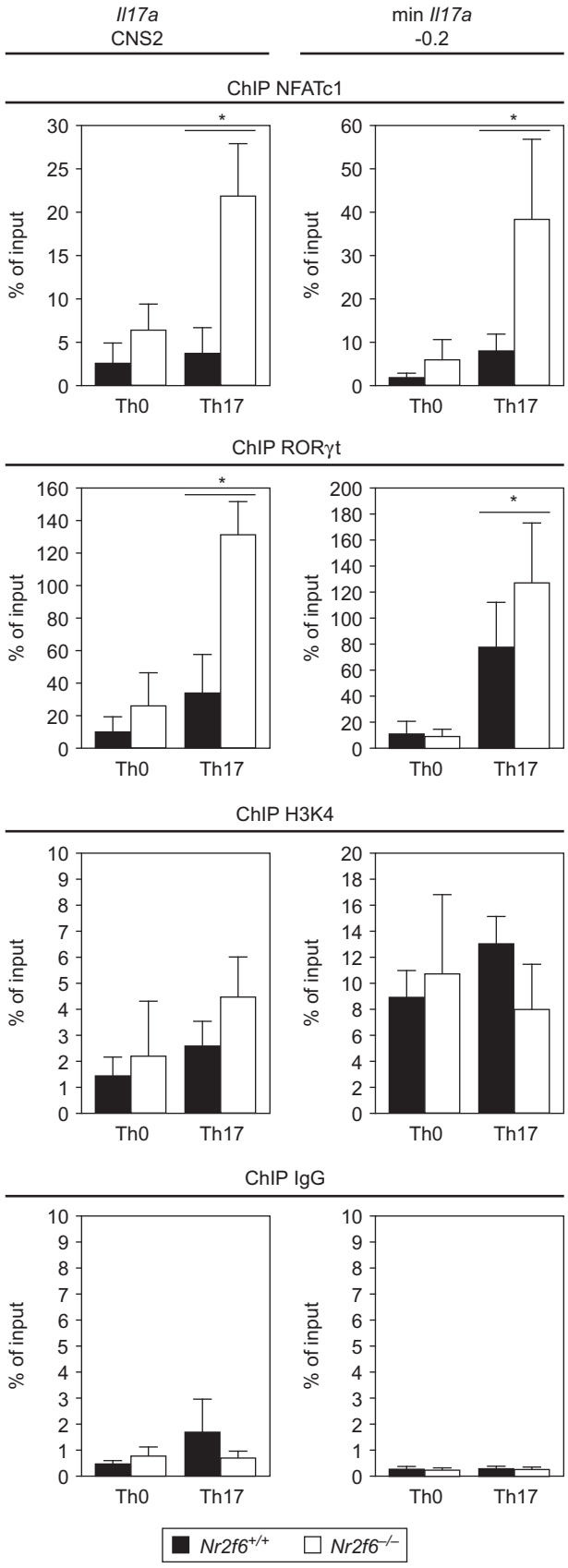

Fig. 7. Loss of NR2F6 enhances NFAT and RORγt binding capabilities at the *Il17a* promoter locus. ChIP analysis of naïve *Nr2f6*$^{+/+}$ or *Nr2f6*$^{-/-}$ CD4^{+} T cells stimulated under Th0 or Th17 conditions for 3 days, then stimulated with αCD3 ON, crosslinked with formaldehyde and immunoprecipitated with anti-NFATc1, anti-RORγt, anti H3K4 or anti-IgG. Bound DNA was amplified by quantitative PCR using primers from either the minimal *Il17a* promoter locus (−0.2 kb, and 0.9 kb [8]) or the CNS2 *Il17a* promoter locus (−5 kb) [16], and the results are presented relative to the input DNA. The IgG background levels are shown. Data are pooled from three independent experiments. The error bars denote the mean ± s.e.m. $^{*}p < 0.05$.

NR2F6 directly interacts with NFAT in a DNA scaffold-dependent fashion, which is in contrast to the mechanism proposed for the vitamin D receptor (VDR), whereby the VDR directly competes with NFATc1 binding to the two binding sites within the human minimal *Il17a* promoter [39].

We propose that the functionally important interaction between NR2F6 and NFAT occurs upon suboptimal antigen stimulation in CD4^{+} T cells. Moreover, NR2F6-NFAT sequestration may be the mechanism by which NR2F6 blocks NFAT-mediated *Il17a* transactivation to prevent exaggerated *Il17a* expression and the subsequent inflammatory response. Along this line of reasoning, Santalasci et al. [40] have shown recently that *NFATc1*, as well *JUN* and *FOS*, mRNA levels are significantly lower in human Th17 cells than in the Th1 subset.

Il21 expression, which is also highly dependent on the activation of the transcription factor NFAT [41–43] is also exaggerated in *Nr2f6*-deficient Th17 CD4^{+} T cells, although the detailed molecular mechanism responsible remains to be elucidated. In fact, most of the molecular mechanisms responsible for the effects of nuclear receptor ligands and/or cell-specific nuclear receptor deletion have not been determined [27]; in particular, it is unclear how specificity is achieved despite highly homologous hormone response (HRE) DNA-binding core consensus sequences. PPARγ suppresses Th17 differentiation by directly interfering with the silencing mediator of retinoid acid and thyroid hormone receptor (SMRT) clearance from the *Rorc* promoter. Therefore, PPARγ activation suppresses not only the expression of *Rorc* but also that of *Il17a*, *Il17f*, *Tnfa*, *Il22*, *Il21*, *Il23r*, *CCR6* and *CCL20* [18]. LXRα (NR1H3) and LXRβ (NR1H2) negatively regulate Th17 differentiation through the activation of sterol regulatory element binding protein 1 (Srebp-1), which subsequently binds to the *Il17a* promoter and directly interferes with Ahr transactivation [17,44]. LXR reduces the expression of *Rorγt*, *Il17a*, *Il17f*, *Il22*, *Il23r* and *Ahr* but does not affect that of *Il21* and *Rora*. RAR suppresses Th17 differentiation through retinoic acid-mediated inhibition of *Il23r*, *Il6r* and *Irf4* expression and Smad2/3 phosphorylation via the TGFβ receptor pathway [45]. The vitamin D receptor (VDR), either alone or in combination with RXR, directly competes with NFATc1 binding to the two binding sites within the human minimal *Il17a* promoter, recruits histone deacetylases and sequesters Runx1 from its binding sites under activating conditions [39]. RORγ and RORα are the linage-specific transcriptional activators of the Th17 subset; these factors bind as monomers and potently upregulate *Il17* transcription [41]. RORE consensus binding sequences have been identified by independent groups at the minimal *Il17a* promoter region as well as the CNS2 region 5 kb upstream of the transcription start [5,7,19,41,46]. Wang et al. [5] have recently reported that the binding of RORγt (and RORα) to the CNS2 region is necessary to initiate chromatin remodeling and the subsequent transcriptional activation of the *Il17a–Il17f* locus in CD4^{+} Th17 cells. Foxp3 inhibits RORγt transactivation through a DNA-independent, direct physical interaction [47]. However, both the RORγt and Foxp3 transcription factors are regulated by Runx1, which also binds within the minimal *Il17a* promoter region and binds directly to RORγt, thereby enhancing *Il17a* transcription [7].

We have shown that NR2F6 directly binds to these RORE sites within the *Il17a* locus and subsequently interferes with the transactivation of the *Il17a* promoter. In *Nr2f6*-deficient Th17 CD4^{+} T cells, RORγt binding was strongly enhanced, particularly at the

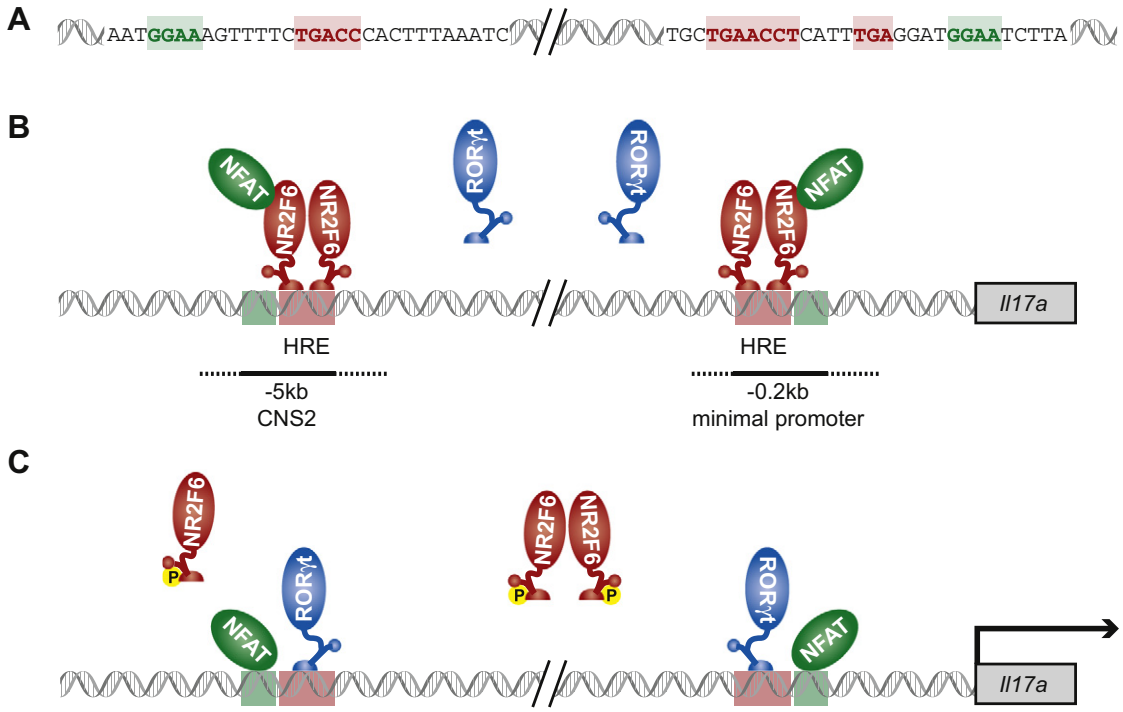

Fig. 8. Regulation of *Il17a* transcription by NR2F6. (A) DNA consensus binding sequences within the minimal and the CNS2 region of the *Il17a* promoter for NFAT (green) as well as for nuclear receptors as NR2F6 and RORγt (red) are shown. (B) In the absence or low affinity TCR stimulation NR2F6 binds to the HRE within the *Il17a* minimal and the CNS2 region, thereby NR2F6 physically blocks NFAT and/or RORγt access to their DNA binding sequences and transcription of *Il17a* is not initiated. (C) In TCR stimulated T cells, NR2F6 is phosphorylated by PKC in the nucleus [18] and thereby loses its DNA binding capacity, subsequently NFAT and RORγt are able to bind to their consensus sequences and mediate the transcription of *Il17a*.

CNS2 region, whereas the overexpression of NR2F6 suppressed RORγt DNA binding. To our knowledge, these data represent the first example of two nuclear orphan receptors with opposing functions binding to the same HRE elements within the *Il17a* locus. The concept that related transcription factors can bind the same elements within the *Il17a* locus has already been demonstrated for STAT3 and STAT5 [48]. However, in contrast to the opposing roles of the STAT family members, which are activated by the cytokine receptors IL-2R and IL-6R, respectively, NR2F6 binds to the HRE in resting cells.

Despite emerging evidence for the key role of nuclear receptor signaling in the regulation of Th17 cell differentiation and function, the molecular mechanisms responsible have remained elusive. The results presented here suggest that in contrast to the nuclear receptors that inhibit Th17 differentiation in a receptor activation-dependent way, such as PPARγ, VDR, RAR, ER and LXR, NR2F6 is prebound to the *Il17a* locus. Only after stimulation-dependent displacement of NR2F6 from the *Il17a* locus can the transcription factors RORγt and NFAT bind to their *Il17a* promoter consensus sequences and subsequently initiate *Il17a* transcription.

5. Conclusion

Our work unravels the molecular mechanisms underlying how NR2F6 attenuates the DNA accessibility of NFAT and RORγt, ensuring the proper level of *Il17a* promoter activation and identifies NR2F6 as a gatekeeper for the transcriptional suppression of *Il17a* in Th17 cells. In contrast to RORγt, which is activated by the cytokines TGFβ and IL-6 in combination with the TCR, NR2F6 already binds to the HRE at the *Il17a* locus in resting cells as a barrier against autoimmunity. Given the reported key role of the IL-17 in autoimmune diseases, our report closes an important gap in the understanding of how the expression of this cytokine is controlled via NR2F6. These findings support the idea that selective activation of NR2F6 could represent an innovative therapeutic regimen for attenuating IL-17A production as a treatment for certain Th17-mediated autoimmune disorders.

Acknowledgment

This work was supported by grants from the FWF Austrian Science Fund (P23537-B13, SFB-021, MCBO-DK), the European Community Seventh Framework Program SYBILLA under grant agreement n°HEALTH-F4-2008-201106, and the Medical University Innsbruck grant (MUI-Start1 2010011001). We are grateful to H. Dietrich, N. Krumböck, and G. Böck (all from Innsbruck) for their technical assistance. Special thanks go to Gaffen-S, Takayanagi-H as well as Takaesu-G for providing different *Il17a* promoter plasmid constructs.

References

[1] Korn T, Bettelli E, Oukka M, Kuchroo VK. IL-17 and Th17 cells. Annual Review of Immunology 2009;27:485–517.
[2] Veldhoen M, Stockinger B. TGFbeta1, a "Jack of all trades": the link with pro-inflammatory IL-17-producing T cells. Trends in Immunology 2006;27:358–61.
[3] Dong C. TH17 cells in development: an updated view of their molecular identity and genetic programming. Nature Reviews Immunology 2008;8:337–48.
[4] Harrington LE, Hatton RD, Mangan PR, Turner H, Murphy TL, Murphy KM, et al. Interleukin 17-producing $CD4^+$ effector T cells develop via a lineage distinct from the T helper type 1 and 2 lineages. Nature Immunology 2005;6:1123–32.
[5] Wang X, Zhang Y, Yang XO, Nurieva RI, Chang SH, Ojeda SS, et al. Transcription of Il17 and Il17f is controlled by conserved noncoding sequence 2. Immunity 2012;36:23–31.

[6] Akimzhanov AM, Yang XO, Dong C. Chromatin remodeling of interleukin-17 (IL-17)-IL-17F cytokine gene locus during inflammatory helper T cell differentiation. The Journal of Biological Chemistry 2007;282:5969–72.
[7] Zhang F, Meng G, Strober W. Interactions among the transcription factors Runx1, RORγt and Foxp3 regulate the differentiation of interleukin 17-producing T cells. Nature Immunology 2008;9:1297–306.
[8] Schraml BU, Hildner K, Ise W, Lee WL, Smith WA, Solomon B, et al. The AP-1 transcription factor Batf controls T(H)17 differentiation. Nature 2009;460:405–9.
[9] Gomez-Rodriguez J, Sahu N, Handon R, Davidson TS, Anderson SM, Kirby MR, et al. Differential expression of interleukin-17A and -17F is coupled to T cell receptor signaling via inducible T cell kinase. Immunity 2009;31:587–97.
[10] Okamoto K, Iwai Y, Oh-Hora M, Yamamoto M, Morio T, Aoki K, et al. IkappaBzeta regulates T(H)17 development by cooperating with ROR nuclear receptors. Nature 2010;464:1381–5.
[11] Zhou L, Littman DR. Transcriptional regulatory networks in Th17 cell differentiation. Current Opinion in Immunology 2009;21:146–52.
[12] Ghoreschi K, Laurence A, Yang XP, Tato CM, McGeachy MJ, Konkel JE, et al. Generation of pathogenic T(H)17 cells in the absence of TGF-beta signalling. Nature 2010;467:967–71.
[13] Chung Y, Chang SH, Martinez GJ, Yang XO, Nurieva R, Kang HS, et al. Critical regulation of early Th17 cell differentiation by interleukin-1 signaling. Immunity 2009;30:576–87.
[14] Li L, Ruan Q, Hilliard B, Devirgiliis J, Karin M, Chen YH. Transcriptional regulation of the Th17 immune response by IKK(alpha). The Journal of Experimental Medicine 2011;208:787–96.
[15] Wei G, Wei L, Zhu J, Zang C, Hu-Li J, Yao Z, et al. Global mapping of H3K4me3 and H3K27me3 reveals specificity and plasticity in lineage fate determination of differentiating $CD4^+$ T cells. Immunity 2009;30:155–67.
[16] Yang XO, Pappu BP, Nurieva R, Akimzhanov A, Kang HS, Chung Y, et al. T helper 17 lineage differentiation is programmed by orphan nuclear receptors ROR alpha and ROR gamma. Immunity 2008;28:29–39.
[17] Veldhoen M, Hocking RJ, Atkins CJ, Locksley RM, Stockinger B. TGFbeta in the context of an inflammatory cytokine milieu supports de novo differentiation of IL-17-producing T cells. Immunity 2006;24:179–89.
[18] Hermann-Kleiter N, Gruber T, Lutz-Nicoladoni C, Thuille N, Fresser F, Labi V, et al. The nuclear orphan receptor NR2F6 suppresses lymphocyte activation and T helper 17-dependent autoimmunity. Immunity 2008;29:205–16.
[19] Zhou L, Lopes JE, Chong MM, Ivanov II , Min R, Victora GD, et al. TGF-beta-induced Foxp3 inhibits T(H)17 cell differentiation by antagonizing RORγt function. Nature 2008;453:236–40.
[20] Chen JF, Yao ZX. The progresses of research on SOCS family in the central nervous system. Sheng Li Ke Xue Jin Zhan: Progress in Physiology 2006;37:108–12.
[21] Ichiyama K, Sekiya T, Inoue N, Tamiya T, Kashiwagi I, Kimura A, et al. Transcription factor Smad-independent T helper 17 cell induction by transforming-growth factor-beta is mediated by suppression of eomesodermin. Immunity 2011;34:741–54.
[22] Moisan J, Grenningloh R, Bettelli E, Oukka M, Ho IC. Ets-1 is a negative regulator of Th17 differentiation. The Journal of Experimental Medicine 2007;204:2825–35.
[23] Mathur AN, Chang HC, Zisoulis DG, Kapur R, Belladonna ML, Kansas GS, et al. T-bet is a critical determinant in the instability of the IL-17-secreting T-helper phenotype. Blood 2006;108:1595–601.
[24] Gocke AR, Cravens PD, Ben LH, Hussain RZ, Northrop SC, Racke MK, et al. T-bet regulates the fate of Th1 and Th17 lymphocytes in autoimmunity. Journal of Immunology 2007;178:1341–8.
[25] Zhu J, Davidson TS, Wei G, Jankovic D, Cui K, Schones DE, et al. Down-regulation of Gfi-1 expression by TGF-beta is important for differentiation of Th17 and $CD103^+$ inducible regulatory T cells. The Journal of Experimental Medicine 2009;206:329–41.
[26] Maruyama T, Li J, Vaque JP, Konkel JE, Wang W, Zhang B, et al. Control of the differentiation of regulatory T cells and T(H)17 cells by the DNA-binding inhibitor Id3. Nature Immunology 2011;12:86–95.
[27] Glass CK, Saijo K. Nuclear receptor transrepression pathways that regulate inflammation in macrophages and T cells. Nature Reviews Immunology 2010;10:365–76.
[28] Nolting J, Daniel C, Reuter S, Stuelten C, Li P, Sucov H, et al. Retinoic acid can enhance conversion of naive into regulatory T cells independently of secreted cytokines. The Journal of Experimental Medicine 2009;206:2131–9.
[29] Klotz L, Burgdorf S, Dani I, Saijo K, Flossdorf J, Hucke S, et al. The nuclear receptor PPAR gamma selectively inhibits Th17 differentiation in a T cell-intrinsic fashion and suppresses CNS autoimmunity. The Journal of Experimental Medicine 2009;206:2079–89.
[30] Chen Z, Laurence A, Kanno Y, Pacher-Zavisin M, Zhu BM, Tato C, et al. Selective regulatory function of Socs3 in the formation of IL-17-secreting T cells. Proceedings of the National Academy of Sciences of the United States of America 2006;103:8137–42.
[31] Hirota K, Duarte JH, Veldhoen M, Hornsby E, Li Y, Cua DJ, et al. Fate mapping of IL-17-producing T cells in inflammatory responses. Nature Immunology 2011;12:255–63.
[32] Miller SD, Karpus WJ. Experimental autoimmune encephalomyelitis in the mouse. In: Coligan John E, et al., editors. Current protocols in immunology; 2007 [Chapter 15:Unit 15 1].
[33] Axtell RC, de Jong BA, Boniface K, van der Voort LF, Bhat R, De Sarno P, et al. T helper type 1 and 17 cells determine efficacy of interferon-beta in multiple sclerosis and experimental encephalomyelitis. Nature Medicine 2010;16:406–12.
[34] Korn T, Reddy J, Gao W, Bettelli E, Awasthi A, Petersen TR, et al. Myelin-specific regulatory T cells accumulate in the CNS but fail to control autoimmune inflammation. Nature Medicine 2007;13:423–31.
[35] Liu XK, Lin X, Gaffen SL. Crucial role for nuclear factor of activated T cells in T cell receptor-mediated regulation of human interleukin-17. The Journal of Biological Chemistry 2004;279:52762–71.
[36] Carey MF, Peterson CL, Smale ST. Chromatin immunoprecipitation (ChIP). Cold Spring Harbor Protocols 2009; 2009:pdb prot5279.
[37] Gruber T, Hermann-Kleiter N, Hinterleitner R, Fresser F, Schneider R, Gastl G, et al. PKC-theta modulates the strength of T cell responses by targeting Cbl-b for ubiquitination and degradation. ra30. Science Signaling 2009;2.
[38] Ghosh S, Koralov SB, Stevanovic I, Sundrud MS, Sasaki Y, Rajewsky K, et al. Hyperactivation of nuclear factor of activated T cells 1 (NFAT1) in T cells attenuates severity of murine autoimmune encephalomyelitis. Proceedings of the National Academy of Sciences of the United States of America 2010;107:15169–74.
[39] Joshi S, Pantalena LC, Liu XK, Gaffen SL, Liu H, Rohowsky-Kochan C, et al. 1,25-dihydroxyvitamin D(3) ameliorates Th17 autoimmunity via transcriptional modulation of interleukin-17A. Molecular and Cellular Biology 2011;31:3653–69.
[40] Santarlasci V, Maggi L, Capone M, Querci V, Beltrame L, Cavalieri D, et al. Rarity of human T helper 17 cells is due to retinoic acid orphan receptor-dependent mechanisms that limit their expansion. Immunity 2012;36:201–14.
[41] Mehta DS, Wurster AL, Weinmann AS, Grusby MJ. NFATc2 and T-bet contribute to T-helper-cell-subset-specific regulation of IL-21 expression. Proceedings of the National Academy of Sciences of the United States of America 2005;102:2016–21.
[42] Spolski R, Kashyap M, Robinson C, Yu Z, Leonard WJ. IL-21 signaling is critical for the development of type I diabetes in the NOD mouse. Proceedings of the National Academy of Sciences of the United States of America 2008;105:14028–33.
[43] Spolski R, Leonard WJ. The Yin and Yang of interleukin-21 in allergy, autoimmunity and cancer. Current Opinion in Immunology 2008;20:295–301.
[44] Cui G, Qin X, Wu L, Zhang Y, Sheng X, Yu Q, et al. Liver X receptor (LXR) mediates negative regulation of mouse and human Th17 differentiation. The Journal of Clinical Investigation 2011;121:658–70.
[45] Xiao S, Jin H, Korn T, Liu SM, Oukka M, Lim B, et al. Retinoic acid increases $Foxp3^+$ regulatory T cells and inhibits development of Th17 cells by enhancing TGF-beta-driven Smad3 signaling and inhibiting IL-6 and IL-23 receptor expression. Journal of Immunology 2008;181:2277–84.
[46] Ichiyama K, Yoshida H, Wakabayashi Y, Chinen T, Saeki K, Nakaya M, et al. Foxp3 inhibits RORγt-mediated IL-17A mRNA transcription through direct interaction with RORγt. The Journal of Biological Chemistry 2008;283:17003–8.
[47] Zhou H, Li WM, Zhang M, Liu ZR, Zou P. Foxp3-transfected $CD4^+$ CD25- T cells suppress function of dendritic cells. Zhongguo Shi Yan Xue Ye Xue Za Zhi/Zhongguo Bing Li Sheng Li Xue Hui: Journal of Experimental Hematology/Chinese Association of Pathophysiology 2008;16:164–9.
[48] Yang XP, Ghoreschi K, Steward-Tharp SM, Rodriguez-Canales J, Zhu J, Grainger JR, et al. Opposing regulation of the locus encoding IL-17 through direct, reciprocal actions of STAT3 and STAT5. Nature Immunology 2011;12:247–54.